ESTIMATION OF THE RESIDUAL STRESS STATE GENERATED DURING THE CURING OF A THICK EPOXY MATRIX BY PULSED LASER

Ch. Jochum [a*], M. Arrigoni [a], M. Boustie [b], J.C. Grandidier [b],

[a] *Mechanics of Naval & Offshore Structures, ENSTA Bretagne LBMS/EA 4325, Brest, France*
[b] *Institut P' CNRS, ENSMA/Université de Poitiers, Futuroscope, France*
**christian.jochum@ensta-bretagne.fr*

Keywords: FEM, curing, epoxy, pulsed laser.

Abstract
This work presents an extension of the pulsed laser shock approach to assess the internal stress level of the matrix at the end of the process. The cut-off fracture technique, based on the maximal tensile stress for instance, is used for shock simulation results analysis, thanks to epoxy failure criteria. Identifications of damage area within thick epoxy samples after a laser shock are also performed to assess simulation results for damage prediction.

1 Introduction

High performance epoxies are more and more used for structural applications, namely for naval and offshore structures as well as for aeronautical and aerospace structures. It is well known today that internal residual stresses are developed during the curing of thermosetting materials. However, several defects like cracks and bubbles inside of the matter might arise, especially with increasing thickness. These defects may provoke serious damages within the structure in service, especially under dynamic solicitations. In order to offer a better quality control, pulsed lasers have recently been used in non destructive inspection and characterization of composites [1]. This work focuses on internal gradients of properties generated during the curing and their consequences on the dynamical behavior of the LY 556® epoxy. Couplings induced by the curing between the chemistry, the thermal and the mechanics of the matrix in progress are presented and are taken into account for a spatial description within the matrix. This paper presents therefore simulation results for a 32 mm thick epoxy cylinder, exposed to laser induced shock waves, by taken into account internal gradients of properties induced by the curing.

2 The LY556 epoxy curing model

The resin system tested in this study is a three-component anhydride-epoxy system from Ciba. The blend consists of a bifunctional DGEBA-type epoxy (Araldite LY556, EEW=183-192 g/eq, n=0.3), a tetra-functionnal anhydride hardener (methyl-tetrahydrophthalic anhydride HY 917, anhydride equivalent weight = 166g/eq), and an accelerator (l-methyl imidazole DY 070). The components were mixed in LY 556/HY 917/DY 070 weight ratio of 100/90/1, resulting in a stoichiometric epoxy-anhydride mixture.

2.1 The LY556 epoxy curing model

As the curing evolves, the chemical degree of conversion rate is less and less important and the thermosetting reaction becomes diffusion controlled [2]. Thus, a semi-empirical relationship (1) proposed by Fournier et al. and based on free volume consideration, was chosen for the description of diffusion effects. Fournier et al. extended the Kamal and Sourour model by a diffusion factor $f_d(\alpha)$ as presented by equation (1):

$$\frac{d\alpha}{dt} = (K_1 + K_2\,\alpha^m)(1-\alpha)^n f_d(\alpha)\ ;\ f_d(\alpha) = \left[\frac{2}{(1+\exp[(\alpha-\alpha_f)/b])} - 1\right]\ ;\ K_1 = A_1\exp\left(\frac{-E_1}{RT}\right)\ ;\ K_2 = A_2\exp\left(\frac{-E_2}{RT}\right) \qquad (1)$$

α_f is the degree of conversion measured at the end of a given isothermal curing and b is an empiric diffusion constant of the material. The methodology for cure kinetics identification with diffusion effects is detailed in [3] and results for the LY 556 epoxy are presented in Table 1. and Table 2.

A_1 (s^{-1})	A_2 (s^{-1})	E_1 (kJ/mol)	E_2 (kJ/mol)
1339879.17	21042820.69	69.14	72.62
m = 1 ; n = 2			

Table 1. Cure kinetics coefficients of the LY556 epoxy resin system for the Kamal and Sourour model

b=7.1588 E-4.T(°K) – 2.2816 E-1	α_f =4.0646 E-3.T(°K) – 8.2434 E-1

Table 1. Temperature dependency of diffusion parameter b and final degree of conversion α_f for the LY556 epoxy resin system.

2.2 Solving of the thermal, chemical and mechanical problem during the curing

The local temperature T of the matrix during the curing is defined by following equation of heat transfer:

$$\rho\,\mathbf{Cp}\frac{dT}{dt} = -\,\mathrm{div}\{\boldsymbol{\lambda}_T\,[-\overrightarrow{\mathrm{grad}}\,T]\} + r + \rho\,\mathbf{\Delta H^r}\,d\boldsymbol{\alpha}/dt - T\,\{(3\boldsymbol{\lambda} + 2\boldsymbol{\mu})\,\boldsymbol{\alpha}_T\}\,\mathrm{tr}\,\dot{\underline{\underline{\varepsilon}}}^e \qquad (2)$$

where Cp, λ_T, ρ and r stand respectively for specific heat, thermal conductivity, density and heat radiation imposed by the oven. α_T is the coefficient of thermal expansion (CTE) of the matrix in formation. λ and μ are the Lamé coefficients of the matrix. Nevertheless, with increasing thickness, mass effect of the epoxy has to be taken into account because of the exothermal aspect of the thermosetting reaction. This statement is clearly demonstrated by equation of heat transfer (2) where the coupling between the thermal and the chemistry appears.

Precise details of the numerical solving strategy were presented by the author in a previous work [2]. This solving strategy was applied to a cylindrical block of resin (diameter 32 mm, height 30 mm) cured in a steel tube with a thickness of 6mm. The heating of the steel tube containing the liquid resin was reproduced by FEM analysis. A special attention was given to the determination of the convection interaction determination between the steel test tube and the air of the oven in order to reproduce as realistic as possible a real condition of oven heating that corresponds to a 3°C/min ramp followed by a 100°C plateau, for instance. Due to the axial symmetry of the structure the mesh was performed with 8-node thermally coupled axisymmetric solid, biquadratic displacement, bilinear temperature CAX8T elements of the Abaqus® element library. The full model requires 240 elements and 787 nodes for results convergence. The computation time takes around 25 min on a Pentium IV HT desktop at 3.20 GHz with 2Go of Ram.

3 Results for cure coupling effects on epoxy matrix state

3.1 Temperature and degree of cure history

The FEM solving technique led to the prediction of gradients of temperature developed within the epoxy during the cure, hence gradients of properties, which are significant as shown in Fig.2 for cure conversion and in Fig.1 for temperature history. Corresponding first internal stress level observed were found around 10 MPa which is significant at the hot stage of the curing, before the cooling step.

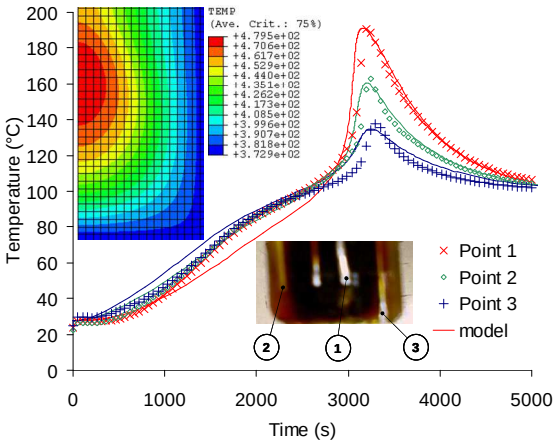

Figure 1. Temperature history during the curing in a 30 mm thick epoxy; comparison between model and thermocouple probes inside of the epoxy matrix (LY556 epoxy resin, ramp 3°C/min and 100°C plateau).

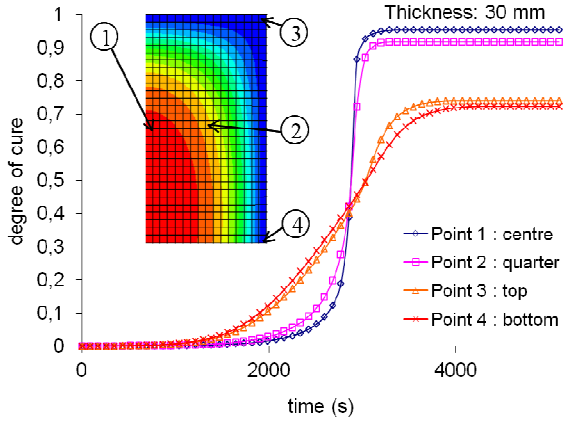

Figure 2. Degree of cure gradients predicted within a 30mm thick epoxy matrix during the 3°C/min ramp and 100°C plateau.

3.2 Properties gradients after the curing

It is assumed here that the thermal and chemical coupling problem is the main leading coupling to take into account, as exposed in [2]. Thus heat generated by the strain rate, as mentioned in equation of heat transfer (2) was considered as a second order effect. This assumption was validated by the solving of the thermal an chemical coupling only, presented in equation (2), that fits well internal temperature history prediction during the curing as shown in Fig. 3. Consequently, all mechanical parameters like Young modulus, bulk modulus, shear modulus, yield stress, failure stress could be considered as being dependent of degree of cure and temperature only.

3.2.1 Elastic, shear and bulk modulus E, G' and K

Elastic modulus E was deduced from shear modulus and Poisson ratio of the cured matrix that is supposed to be locally isotropic and homogeneous. Shear tests were performed on pure epoxy matrix samples as shown in Fig. 3. A video controlled shear technique was used and led to the plot of local shear stress versus local strain. Video controlled shear tests were performed at different temperature to account for rubbery or glassy state behaviors of the matrix. Results are shown in Fig. 4. It is pointed out that elastic shear modulus was found to be around 10 MPa. in the rubbery state and increases strongly in the glassy state to a level of 1000 MPa. at room temperature. Thus, for a fully cured epoxy (~90% of degree of cure), shear modulus evolution versus temperature is summarized in Fig. 5.

A linear mixture rule relation, based on the degree of conversion α, was used for G' modulus description as follows:

$$G'(\alpha,T) = (1-\alpha).\, G'liq + \alpha\, G'fully\ cured(T) \qquad (3)$$

Where elastic modulus in liquid state G'_{liq} ~100Pa. [4] and the fully cured modulus $G'_{fully\ cured}$ is given by Fig. 5. A strong change is logically observed at Tg crossing. This sophistication was taken into account for the determination of G' obtained at the end of the hot stage before cooling, thanks to Tg modeling given by the usual Pascault and Williams relation (also called Di-Benedetto equation). Details are available in [2].

The linear mixture rule approach was also applied to the bulk modulus K, but without any sophistication at Tg crossing assuming no changes there. After cooling to room temperature, the epoxy matrix is in a fully glassy state. However, degree of cure gradient exists within the matrix. Consequently gradient of shear modulus is developed as shown in Fig. 6 along cylinder axis.

Figure 3. Shear test done at 125°C. The white spot was used for video-control of strain evolution. Plasticity is obtained after cooling.

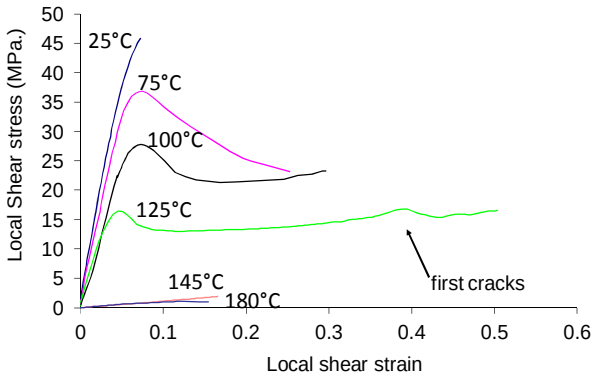

Figure 4. Local shear stress strain evolutions versus temperature.

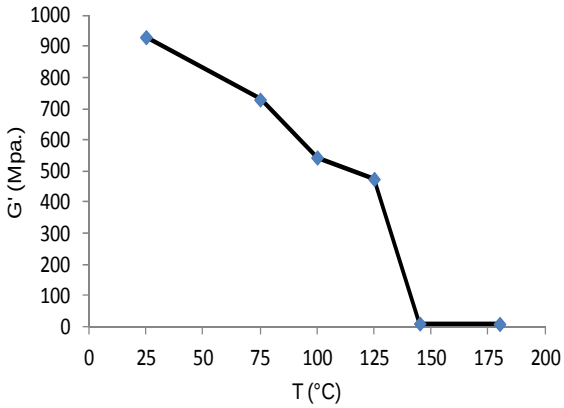

Figure 5. Epoxy Elastic shear modulus change with temperature (~fully cured epoxy).

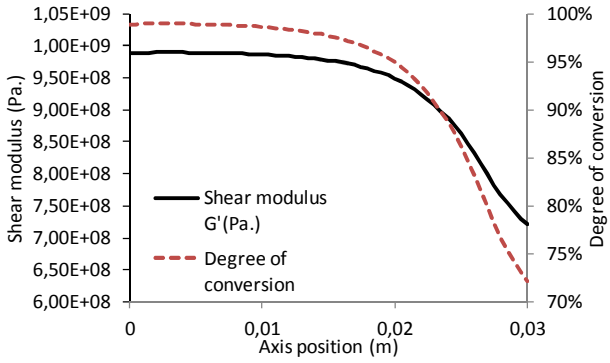

Figure. 6. Elastic shear modulus and degree of conversion gradients at room temperature, along cylinder axis.

3.2.2 Young modulus, Poison ratio and density

Poisson ration was deduced from elastic shear and bulk moduli, assuming locally an isotropic behaviour. Density was deduced from the Li et al. Cure shrinkage model applied to the LY 556 epoxy, details are available in [2]. Young modulus was then calculated thanks to shear modulus and Poisson ratio and results are shown in Fig. 7.

3.2.3 Yield and failure stress description

Yield stress was obtained on a fully cured epoxy sample thanks to the video controlled shear tests presented in Fig. 3. It was then assumed that the yield stress evolution within the matrix, after return at room temperature, could be directly described by a linear dependency to the fully cured yield stress thanks to the local degree of conversion obtained after the curing. Evolution along the axis of the cylinder of epoxy is shown in Fig. 8.

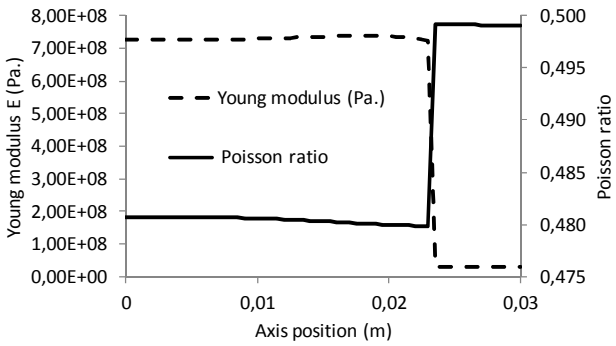

Figure 7. Epoxy Elastic shear modulus change with temperature.

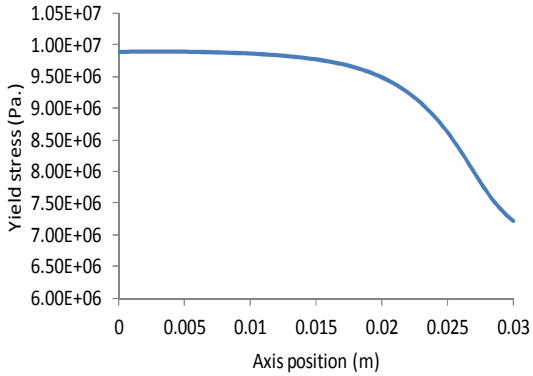

Figure 8. Yield shear stress change along the axis of the cylinder block of epoxy, at room temperature.

Failure stress is more delicate to model according to shear stress strain curves where plasticity clearly exists. Nevertheless, as video controlled shear tests were conducted up to the macroscopic failure of the sample, fail stress given here stands for macroscopic failure stress. Failure stress was then described in the same manner as for yield stress but ranging from 95 to 130 MPa.

4 Non destructive characterization of thick epoxy by pulsed laser technique

The dynamic behavior of composites under laser ultrasonics or laser induced shock waves is becoming a matter of interest [[1], [5]]. In these studies, Numerical models based on finite element methods, and explicit schemes have been proposed. Recently Ecault et al [6] have studied the damage of epoxy under intense laser induced shock waves and gave a model for adhesively bonded composites under shocks. However, none of them considered the preexisting gradient of mechanical characteristics (Young modulus, density, yield limit, Poisson coefficient, …) of thick composites due to the curing stage, that vary along the sample thickness during and after the curing. In a previous work, it has been attempted to propose a numerical model supposed to evidence the effects of the gradient of mechanical characteristics on the “time of flight” of a laser induced stress wave on a thick epoxy sample [7].

4.1 Influence of residual stress on time of flight

Numerical simulations, performed with the explicit finite element code RADIOSS®, point out differences of cured epoxy behaviour between homogenous and heterogeneous matrix released at ambient temperature, subjected to hypothetic dynamic loadings. Samples were represented in 32 mm thick epoxy cylinders presented in section 2.2. An axisymetric model, split into 500 elements was used. The element size sensitivity was discussed in the previous work [7]. Two laser spot sizes for inducing the loading were prospected, respectively with radius of 1,5 mm and 3 mm. The behaviour of the ambient material is given by a perfect elastic-plastic model, self consistent for describing the elastic stage. This model is governed by the yield limit Y_0, the Young modulus E and the Poisson coefficient v. In a column of density ρ_0. the free surface velocity signal, in vis a vis of the impact, was of a highest amplitude for the 3 mm spot size. The numerical model of the thick composite was composed of 31 different material layers representing gradients of mechanical properties. Figure 9 shows that the time of flight for a 98 % cured homogeneous epoxy was shorter than the one having gradient of properties (partially cured).

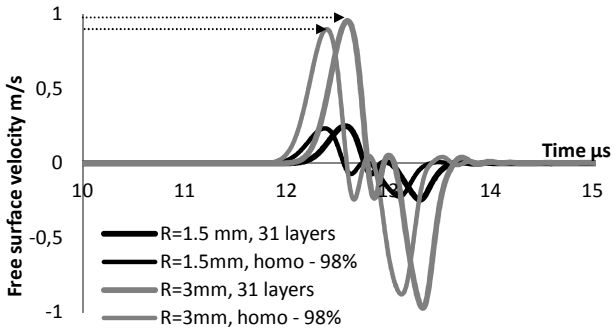

Figure 9. Free surface velocity computed for 98 % degree of cure and 31 layers samples at ambiant temperature. Radius of impact is respectively 1.5 mm in dark lines and 3 mm in grey lines.

4.2 Residual stress evaluation

In order to access to the residual stress, the loading amplitude has been increased up to reach the damage threshold. That is to say that the mechanical behaviour is completed by a hydrodynamic influence composed of the Mie-Grüneisen equation of state $\sigma = -P+\sigma_{dev}$ (4) in which the reference state under dynamic compression is given by the Hugoniot equation of state (5) :

with $P=\Sigma a_i \mu^i$ where $i \leq 3$ and a_i are material coefficients computed with (5) and $\mu=1-\rho/\rho_0$.

$$P - P_{ref} = \frac{\Gamma_0}{\rho_0}(e - e_{ref}) \text{ and } D = C_0 + s(u - u_0) \quad (5)$$

Subscript *ref* refers for the reference state, subscript *0* refers for the initial state, P is the hydrodynamic pressure, e the internal energy, Γ_0 is the Grüneisen coefficient, D the shock velocity, C_0 the bulk sound velocity ans s a Hugoniot coefficient and u the material velocity. Material parameters are presented in table 3. The elasto-plastic formulation coupled with the above equation of state is able to describe the behaviour of the epoxy in elastic regime as well as in plastic (moderate shock) and hydrodynamic regime (intense shock). A “cut-off” damage model acts when the tensile stress comes down to a critical failure stress, depending on the layer, deduced from figure 10 for the multi-layered sample. Two models are compared with a similar impulse loading of 210 MPa. on a 3 mm radius area. The first model is composed of a quasi fully cured (98%) epoxy resin. The second model is a multi layer resin composed of 31 layers which mechanical characteristics evolution along z-axis are given by figures 7 and 8 and summarized in

table 3. Both models are axisymmetric and have lateral absorbing frontiers. Figure 10 shows the difference of damage location between the fully cured (right) and the multilayered sample (left) at 24 µs. The loading is applied on the bottom surface. Simulation results show coherent wave propagation with edge effects that contribute to the damage observed [8]. Crack location is rather close to free surface, which is in accordance with the known damage mechanism under shock [9]

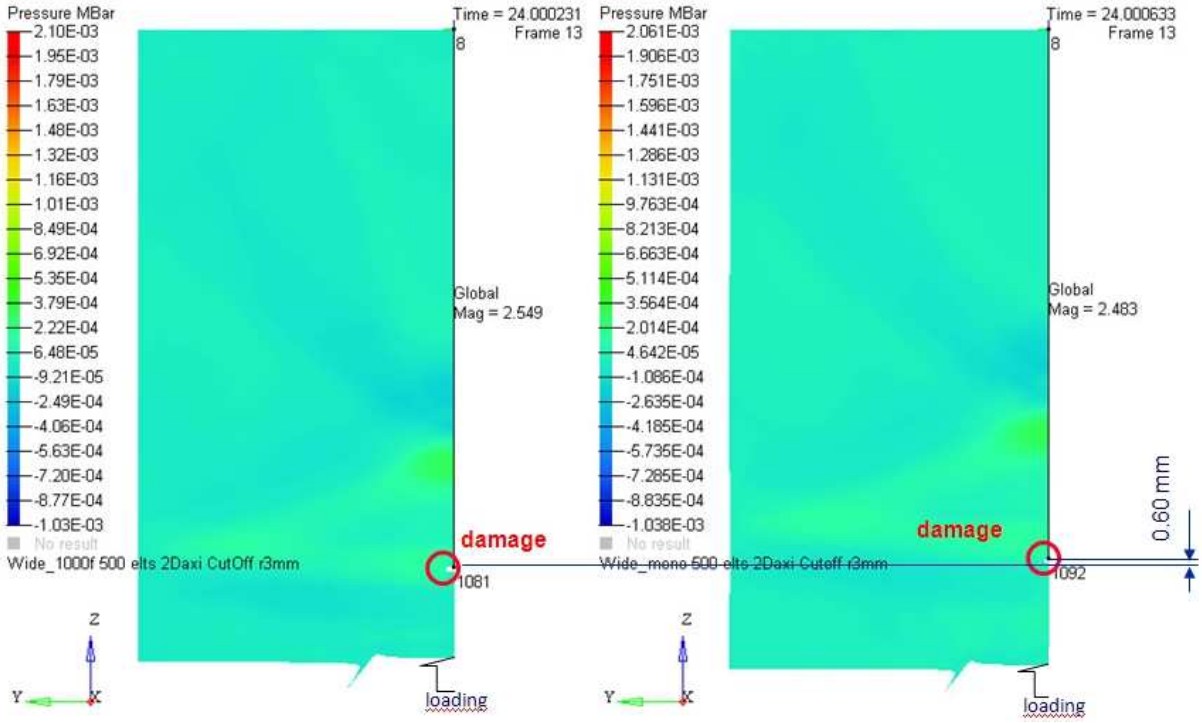

Figure 10. Difference of predicted damage location on multilayered (left) and fully cured sample (right) obtained with RADIOSS®.

The shift in crack position along the z-axis is about 0.6 mm. In the fully cured material, when the cut-off pressure is lower, the damage location is closer to the free surface. When the cut-off pressure is higher, the damage location is more inside the material. The cut-off pressure has been chosen to make damage coincide in both models so that this threshold can be identified as the internal residual stress. The cut-off pressure was found as 13.5±0.5 MPa. This estimation depends of course of the property gradient after curing but is in the same order of magnitude as the value proposed by [[10]], even though the damage model is basic and the material behaviour does not take into account viscous effects.

Degree of curing	80 %	98 %
ρ_0 (g/cm^3)	1.251	1.254
E (MPa)	23.13	28.19
ν	0.432	0.425
C_0	1917	1988
s^{**}	1.47	1.47
Γ_0^*	0.8	0.8
Y_0 (MPa)	8.08	9.89

Table 3. Set of mechanical parameters used in simulations.

5 Conclusions

These preliminary calculations have showed that impact simulation, of bars or laser induced shocks, could lead to determine the degree of cure of a resin released at ambient temperature, by an inverse approach. This numerical work is a predictive step for dimensioning the experimental setup of non destructive experiments that could characterize the gradient of properties within the material at the end of the process.

By a single shot, the response in free surface velocity could be compared to the numerical one, and thus the average state could be estimated. Section 3 showed that the state of the material depends only on degree of cure that would be deduced from the experiment / simulation comparison. By increasing the laser induced shock amplitude, it would also be possible to determine the damage threshold in a thick matrix.

References

[1] E. Gay, L. Berthe, M. Boustie and M. Arrigoni "Experimental study of composite damage under laser shock". Proceedings of 17th *Journées nationale des composites*, Poitiers, France, paper number 168, 15-17 june 2011, (in french).

[2] N. Rabearison, Ch. Jochum and J.C Grandidier, "A FEM coupling model for properties predictions during the curing of an epoxy matrix" *Computational Materials Sciences*, Vol. 45, pp 715–724, 2009.

[3] N. Rabearison, Ch. Jochum and J.-C. Grandidier "A cure kinetics, diffusion controlled and temperature dependent identification of the Araldite LY556 epoxy" *Journal of Materials Science*, Vol. 46, pp. 787-796, 2011.

[4] Ch. Jochum, J.-C. Grandidier and M.A. Smaali, "Proposal for a long-fibre microbuckling scenario during the cure of a thermosetting matrix", *Composites Part A*, Vol. 39, Issue 1, pp. 19-28. 2008.

[5] M. Perton M., A. Blouin A., J.-P. Monchalin, "Adhesive bond strength evaluation in composite materials by laser-generated high amplitude ultrasound » *Journal of Physics*: Conference Series 278 (2011) 012044.

[6] R. Ecault, L. Berthe, M. Boustie, F. Touchard, E. Lescouette, A. Sollier, P. Mercier, J. Benier, "Observation of the shock wave propagation induced by a high-power laser irradiation into an epoxy material*", J. Phys. D:Appl. Phys*. 46 (2013) 235501.

[7] Ch. Jochum, M. Arrigoni, M. Boustie, J.C. Grandidier, "Cure multiphysic couplings effects on the dynamic behaviour of a thick epoxy", *ICCM19*, Montreal July 2013.

[8] M. Boustie., J.-P. Cuq-Lelandais, C. Bolis, L. Berthe, S. Barradas, M. Arrigoni, T. De Resseguier, M. Jeandin, "Study of damage phenomena induced by edge effects into materials under laser driven shocks", *J. Phys. D: Appl. Phys.* 40, p. 7103-7108, (2007).

[9] T. Antoun, L. Seaman, D.R. Curan, G.I. Kanel, S.V. Razorenov and A.V. Utkin 2003 *Spall Fracture (New York: Springer)* 176-97.

[10] Y. Abou-Msallem, N. Boyard, F. Jacquemin, A. Poitou, D.Delaunay and S. Chatel, 2008. Identification of thermal and rheological properties of an aeronautic epoxy resin-simulation of residual stresses. *Int. J. Mater Form Springer, Esaform* 2008, pp:579-58.